Unmixing coral fluorescence emission spectra and predicting new spectra under different excitation conditions

Eran Fux and Charles Mazel

An algorithm was developed that uses prototype spectra and least-squares minimization to unmix the relative contributions of individual pigments to the composite fluorescence emission spectrum of reef corals. Field measurements indicated that it was necessary to include allowance for spectral shift of the wavelength peak of the prototype emission spectra. The unmixed spectra are used to predict the shape and amplitude of composite spectra that would be expected under different excitation conditions. We found that, for cases in which the pigments occur singly or with significant spectral separation, it is necessary to consider the properties of the excitation light sources, only, to make accurate predictions. In cases with spectral overlap the contribution of interpigment coupling cannot be neglected.

OCIS codes: 010.0010, 300.6280.

1. Introduction

Fluorescence can be a powerful tool for probing biological systems. In the marine environment it has been used to great advantage for many years in the detection and investigation of chlorophyll and associated photosynthetic accessory pigments.[1,2] Fluorescence probing is a nondestructive tool that can be applied *in vivo*,[1] *in situ*,[2] or as a remote sensing technique.[3]

When fluorescence is used as a probe, the choice of excitation wavelength is critical to the results. If there is a single pigment of interest it is generally desirable to choose a light source that corresponds to the peak of the fluorescence excitation spectrum to produce the most intense response. The choice becomes more involved when there are multiple sources of fluorescence in a single specimen or when a single fluorescence could arise from energy transfer from more than one light-capturing pigment. In such cases the fluorescence signal that is emitted is very much a function of the excitation light source. This sensitivity of the shape and intensity of the emission spectrum to the excitation wavelength has been exploited as a technique for differentiating macroalgal species.[4]

Corals, the animals responsible for building reefs in tropical regions, contain fluorescent pigments. One of these is chlorophyll, present in symbiotic single-celled algae (dinoflagellates) called zooxanthellae that are found in the coral endodermal tissue. The algae exhibit the deep red (685-nm peak) fluorescence typical of chlorophyll. In addition to algal chlorophyll many corals have fluorescent substances in the animal host tissues. For many years these pigments were the subject of only sporadic interest.[5–7] Recently, however, the number of papers dealing with these pigments has increased dramatically.[8–14] The function of pigments in the coral tissues is still not known. However, one study suggests that coral tissue fluorescence assists zooxanthellae photosynthesis by converting some of the ambient light to wavelengths that are more efficiently absorbed by chlorophyll.[9]

The investigation of coral fluorescence has progressed from the qualitative study of corals in the laboratory to the quantitative measurement of spectral properties of specimens *in situ*.[15,16] A new in-water sensing system, the fluorescence imaging laser-line scanner,[17] has further piqued interest in fluorescence as a method for investigating coral reefs.

As the investigation of coral fluorescence continues, through both imaging and quantitative spectral measurement, it is critical to pay attention to the

E. Fux is with the Department of Ocean Engineering, Massachusetts Institute of Technology, Cambridge, Massachusetts, 02139. The email address for E. Fux is eran@mit.edu. C. Mazel is with Physical Sciences, Inc., 20 New England Business Center, Andover, Massachusetts 01810.

Received 18 May 1998; revised manuscript received 21 September 1998.

0003-6935/99/030486-09$15.00/0

excitation wavelengths used in each study. If this is not done, then it will not be known whether differences in results arise from true differences in response or simply from differences in the excitation wavelengths used.

A recent study[14] indicates that only four pigments other than the symbiotic algal chlorophyll contribute to the fluorescence spectral signatures of Caribbean corals. A coral's fluorescence emission spectrum can result from the excitation of one or more of these pigments. The emission of each of the individual pigments can vary both in intensity and in the precise location of the wavelength peak (data collected to date show variations over a range of ~20 nm for one of the pigments), whereas the shape of the spectrum remains constant. The excitation spectra for these pigments follow the same shifts in wavelength as the emission, maintaining a constant Stokes shift. The emission spectra of several of these pigments strongly overlap, so that it might not always be obvious from the composite spectrum which of the pigments is present and to what degree. The addition of two spectra might also result in apparent shifts in the locations of wavelength peaks.

One of our goals in this study was to develop a mathematical algorithm for separating measured coral fluorescence emission spectra into the contributions of the individual pigments. A second goal was to predict the response produced by any excitation light source, given knowledge of the response produced by a different light source.

2. Method

A. Field Data Collection

Fluorescence spectral data were collected in the summer of 1996 in the Dry Tortugas, Florida. *In situ* fluorescence emission spectra were measured with the benthic spectrofluorometer (BSF), a prototype diver-operated instrument.[15] The BSF utilizes a user-selectable narrow-band (±10 nm FWHM) excitation source and measures emission over the full visible spectrum with a resolution of approximately 10 nm. Data were corrected for dark current and electrical offsets and for the spectral sensitivity of the detector optics. The data were then smoothed with a 17-point Savitzky–Golay[18] smoothing algorithm.

Coral specimens were collected at a depth of 18 m, brought to the surface, and maintained in flowing seawater in the shade. *In vivo* measurements of fluorescence excitation and emission spectra of the intact specimens were made with a FluoroMax-2 spectrofluorometer (Spex Industries) fitted with a fiber-optic adapter. The randomized bifurcated fiber was directed at the surface of a specimen at a 45-deg angle in a darkened enclosure. Excitation and emission spectra were collected with 2-nm bandpass slits. Emission spectra were collected with excitation wavelengths of 365, 450, and 488 nm, at source levels of approximately 47, 78, and 59 $\mu W\ cm^{-2}$, respectively. The acquisition time for a full scan was approximately 30 s. Excitation spectra were collected with the emission monochromator set at 490, 530, 590, and 690 nm. The wavelengths were chosen to define the characteristics of the various coral fluorescent pigments. Emission spectra were corrected with manufacturer-supplied data for relative spectral sensitivity of the detector. We corrected excitation spectra by scanning in the ratio mode. All the scans were corrected for dark current offset. Synchronous scans at 5-nm offset between excitation and emission monochromators were collected to identify which pigments contributed to the measured emission spectrum.

B. Selection of Fluorescence Emission Prototypes

Prior measurements from Caribbean corals[14] identified five constituents, defined by characteristic excitation–emission spectra, of coral fluorescence signals. For lack of a better identification we chose a typical emission peak of each as a naming shorthand and denote these as the 486, 515, 557, 575, and 685 pigments. The 685 pigment is the chlorophyll *a* in the zooxanthellae. All the specimens contained chlorophyll in addition to one or more of the other pigments, but the chlorophyll fluorescence emission peak falls at wavelengths that are of sufficient length that it does not overlap with any of the other emissions. The 557 pigment has been found so far in only one species of coral and is not treated further here.

Prototype spectra were selected for use in the mathematical unmixing routine by identification of specimens that contain only one pigment in the relevant wavelength range. The emission spectra of such samples were trimmed manually to isolate the spectral region of interest. We denote these spectra as end members for the mathematical algorithm.

For the 515 pigment there were enough data (11 spectra) to apply a statistical approach to the selection of the prototype. The spectra were normalized to a peak value of one and were shifted as necessary so that all the peaks fell at 515 nm. The prototype was computed as the mean of these spectra. There was just one sample that contained only the 486 pigment, and that was chosen as the prototype. The 575 pigment never occurred in isolation. An emission spectrum with an especially strong peak in this region was selected to provide the prototype. All the emission prototypes were collected with an excitation wavelength of 488 nm with the exception of the 486 pigment, for which 450 nm was used. The normalized prototype emission spectra are shown in Fig. 1.

A constant dc signal was selected as an additional prototype to account for measurement offsets in the FluoroMax and in the BSF that are most significant in weak signals.

C. Unmixing Algorithm

The unmixing algorithm is based on least-squares minimization.[19,20] Here we introduce the following definitions:

A end members matrix,

x coefficient vector,

b measured sample (vector).

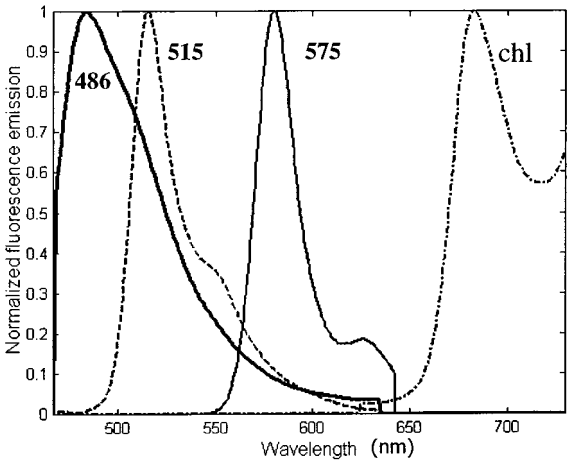

Fig. 1. Normalized prototype emission spectra.

Assume that $b = Ax$ in the absence of noise or measurement errors. Define the squared error between the linear combination of the end members and the measured sample (in matrix notation):

$$e^2 = \|Ax - b\|^2 = (Ax - b)^T(Ax - b). \quad (1)$$

Our goal is to find the vector of coefficients x that minimizes this error. This would give us the combination of end members that is closest to the measured sample. Simplifying Eq. (1) and omitting the constant term yields a quadratic polynomial. For consistency with the solution presented in Ref. 19 the polynomial is divided by two:

$$P = \tfrac{1}{2}x^TA^TAx - x^TA^Tb. \quad (2)$$

The solution that minimizes P is given by[19]

$$A^TAx = A^Tb, \quad (3a)$$

or, in a more convenient form,

$$x = (A^TA)^{-1}A^Tb. \quad (3b)$$

An error index (EI) can be assigned to the solution:

$$\mathrm{EI} = \int_\lambda [b(\lambda) - A(\lambda)x]^2 d\lambda. \quad (4)$$

In our application, the columns of matrix A are the prototype spectra and vector b is the measured spectrum that we wish to unmix to components. The solution vector x contains the weighting factors for each component. The term $(A^TA)^{-1}$ in Eq. (3b) requires that the product A^TA be symmetric positive definite, which in turn requires that the columns of A be linearly independent. Our selection of distinct prototype spectra ensures that the columns in A are independent.

If there were a unique set of end members, the problem would be complete. In practice we observed that, whereas the spectral shape of the individual pigment emissions is nearly constant, the entire curve can be shifted along the wavelength axis over a range as great as 20 nm.[13,14] We must consider all these spectrally shifted variants of the prototypes and decide which combination provides the best solution.

Table 1. Artificial Data Set Used for Testing the Unmixing Algorithm

SET #		1	2	3	4	5	6	7	8
Noise Level		0	0	0	0	0	0	4	8
ORIGINAL	* 486 x	40	40	40	40	40	40	40	40
	515 x	5	5	5	5	5	5	5	5
	575 x	2	2	2	2	2	1**	2	2
	Chl. x	10	10	10	10	10	10	10	10
	486 Shift	0	5	5	5	5	0	5	5
	515 Shift	0	0	-5	-5	-5	5	5	5
	575 Shift	0	0	0	0	5	0	0	0
	Chl. Shift	0	0	0	5	0	-5	5	5
PREDICTED	486 x	40.0000	39.9999	39.9999	39.9963	39.9999	39.7616	40.2706	39.3050
	515 x	4.9995	4.9992	4.9994	5.0073	4.9992	4.8925	5.0890	5.1765
	575 x	1.9972	1.9987	1.9985	1.9722	1.9988	1.0408 **	1.9843	1.9017
	Chl. x	10.0080	10.0079	10.0079	9.6787	10.0079	9.9659	9.8213	9.9983
	486 Shift	0	5	5	5	5	0	5	5
	515 Shift	0	0	-5	-5	-5	5	5	5
	575 Shift	0	0	0	0	5	0	-2	3
	Chl. Shift	0	0	0	5	0	-5	5	5
	Max. Err	0.14%	0.079%	0.079%	3.23%	0.079%	4.08%	1.787%	4.915%

* Read: **486 x** : the 486 prototype multiplier.
486 Shift : the amount (wavelength) by which the 486 prototype curve was shifted.
Original : artificial input values.
Predicted : calculated result from the algorithm.
Max. Err : the largest difference between input and calculated multipliers.

** Set # 6 had DC offset of 1 instead of 575 prototype.

A MATLAB program was written to perform the computations outlined above. The program accepts data files from either the BSF or the FluoroMax-2. Data are interpolated to 1-nm intervals and adjusted to a common wavelength range, with zeros entered if necessary for wavelengths for which there are no data. Equations (3b) and (4) are solved for a given combination of prototypes, and the EI is stored in an error matrix. If a negative value is found for any of the coefficients, its value is set to zero. Each of the first three prototype emission curves (486, 515, and 575) is then shifted in wavelength in a ±10-nm range in 1-nm increments from the initial prototype peak location, for a total of $21 \times 21 \times 21 = 9261$ possible combinations. EI's are calculated for each. The minimal EI represents the combination of weights and shifts that gives the best fit to the sample data.

The chlorophyll emission curve does not overlap with the other three pigments and therefore does not require unmixing. The sample spectrum is scanned from wavelength 650 to 720 nm to find the amplitude and wavelength of the local maximum. The prototype chlorophyll emission curve is then shifted and scaled to match these values.

D. Testing the Unmixing Algorithm

To test the performance of the algorithm, simulated spectra were created by the addition of different

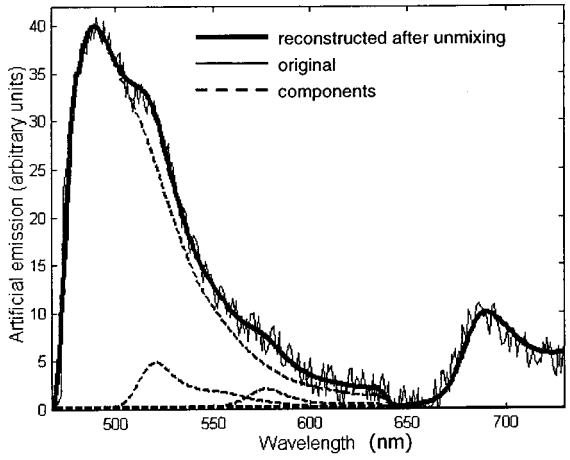

Fig. 2. Artificial test case 7 (Table 1, noise level 10% of signal level).

combinations of the prototype curves. An example of an artificial data set used for testing is described here and summarized in Table 1. We created a representative emission spectrum by weighting the prototype curves by factors of 40, 5, 2, 10, and 0 for the 486, 515, 575, and 685 pigments and the dc offset, respectively. The result was an emission curve similar in shape to those measured from corals in the field. We produced variants of this base spectrum by shifting one or more of the prototype curves on the wavelength axis. A random normally distributed noise was added to two of the spectra at amplitudes 4 and 8, equivalent to 10% and 20%, respectively, of the largest pigment multiplier (this noise was added to simulate BSF data that were collected with a low signal-to-noise ratio, and primarily tests the effectiveness of the smoothing algorithm). A dc offset was added to another spectrum. Figure 2 shows case 7, a simulated spectrum with noise level 4. The unmixing routine was exercised on a variety of test sets of this nature, including cases in which one or more of the pigments were not included in the test spectra and cases in which there were more pigments in the sample than were included in the end members matrix.

The routine was then applied to unmix a number of composite coral spectra from field measurements. Some of the coral samples contained just one of the pigments (in addition to chlorophyll), whereas others contained multiple pigments. After application of the algorithm the unmixed components were combined to create a reconstructed spectrum. The original spectrum was compared with this reconstructed spectrum.

D. Predicted Emission under Different Excitation Conditions

For the following we assume that the fluorescence quantum efficiency (Φ_F) does not depend on excitation wavelength. We define fluorescence quantum efficiency as $\Phi_F(\Delta\lambda_{ex})$ = (total number of photons emitted)/(number of photons absorbed in wavelength band $\Delta\lambda_{ex}$) or

$$\Phi_F(\Delta\lambda_{ex}) = \frac{\int_{\lambda_{em}} f(\lambda_{em})\,d\lambda_{em}}{\int_{\Delta\lambda_{ex}} E_S(\lambda_{ex})a(\lambda_{ex})\,d\lambda_{ex}}, \quad (5)$$

where

$\Phi_F(\Delta\lambda_{ex})$ is the fluorescence quantum efficiency (unitless),
$\Delta\lambda_{ex}$ is the excitation wavelength range (nm),
λ_{em} is the emission wavelength (nm),
$f(\lambda_{em})$ is the fluorescence emission (photons sec^{-1} cm^{-2} nm^{-1}),
E_S is the surface irradiance (photons sec^{-1} cm^{-2} nm^{-1}), and
$a(\lambda)$ is the absorbance of surface at wavelength λ (unitless).

The assumption that fluorescence quantum efficiency is independent of wavelength [$\Phi_F(\lambda_{ex1}) = \Phi_F(\lambda_{ex2})$] yields

$$\int_{\lambda_{em}} f_2(\lambda_{em})\,d\lambda = \frac{\int_{\lambda_{ex2}} E_S(\Delta\lambda_{ex2})a(\Delta\lambda_{ex2})\,d\lambda}{\int_{\lambda_{ex1}} E_S(\Delta\lambda_{ex1})a(\Delta\lambda_{ex1})\,d\lambda} \int_{\lambda_{em}} f_1(\lambda_{em})\,d\lambda, \quad (6)$$

where indices 1 and 2 refer to two different excitation conditions (wavelengths). In practice the absorption spectrum for the fluorescent pigment is unknown. We can measure the excitation spectrum (ex), however, and assume that the two have the same shape.[21]

Equation (6) is the general expression that applies to a source that produces a range of excitation wavelengths. With a narrow-band instrument such as the FluoroMax or a laser source such as is used in the fluorescence imaging laser-line scanner system we can assume that we are dealing with a single excitation wavelength, which enables us to reduce Eq. (6) to

$$\int_{\lambda_{em}} f_2(\lambda_{em})\,d\lambda = \frac{S(\lambda_{ex2})\text{ex}(\lambda_{ex2})}{S(\lambda_{ex1})\text{ex}(\lambda_{ex1})} \int_{\lambda_{em}} f_1(\lambda_{em})\,d\lambda, \quad (7)$$

where $S(\lambda_{ex1})$ and $S(\lambda_{ex2})$ are the source intensities at wavelengths λ_{ex1} and λ_{ex2}, respectively.

With an instrument such as the BSF with a broader-band excitation source we would have to consider the energy distribution over the full range of excitation wavelengths.

A MATLAB routine that uses an algorithm based on Eq. (7) was developed to predict the coral fluorescence emission spectrum that would be excited by wavelength λ_{ex2}, given a measured emission spectrum ex-

cited at wavelength λ_{ex1}. The original spectrum is first unmixed to separate its pigment components. The prediction is applied to each component separately, and the new components are then summed to create the predicted spectrum. The inputs needed to perform the calculation are the relative excitation light source intensities at the two wavelengths and the relative amplitude of the excitation spectrum for each pigment at those wavelengths.

For the 515 and 685 pigments we used a prototype excitation spectrum determined from measurements of specimens that contained only that pigment. The wavelength of the peak of the 515 prototype was adjusted to be 11 nm (the mean Stokes shift for this pigment) shorter than the location of the peak of the emission spectrum of the unmixed 515 component. We did not have enough samples to establish a reliable average prototype for the 486 pigment and used the excitation spectrum measured from the particular sample being processed. For the 575 pigment we used an excitation spectrum from a specimen in which that pigment was dominant.

The prediction algorithm was applied to pairs of spectra measured with the FluoroMax. By use of data measured with an excitation of $\lambda_{ex1} = 365$ nm the prediction was made for the response at $\lambda_{ex2} = 450$ nm and compared with the spectrum measured with that excitation wavelength. A similar analysis was performed for data sets with $\lambda_{ex1} = 450$ nm and $\lambda_{ex2} = 488$ nm. To predict the response of the 486 pigment the procedure could be applied only to the 365 and 450-nm pairs, because 488 nm falls outside this pigment's excitation band.

Not all the measurements that were made in the field were suitable for this analysis. We applied the procedure only to samples that exhibited strong emission responses for the pigment(s) of interest at both excitation wavelengths. We tested four combinations of pigments and excitation conditions:

Three samples processed only for 486 pigment, $\lambda_{ex1} = 365$ nm, $\lambda_{ex2} = 450$ nm.

Four samples containing only 515 pigment, $\lambda_{ex1} = 450$ nm, $\lambda_{ex2} = 488$ nm.

Two samples with both 486 and 515 pigments. The two samples were tested in two modes: $\lambda_{ex1} = 365$ nm, $\lambda_{ex2} = 450$ nm and $\lambda_{ex1} = 450$ nm, $\lambda_{ex2} = 488$ nm.

After we applied the prediction algorithm, we calculated the percentage difference between the predicted emission and the measured emission as the ratio $100 \times$ [(peak value of the predicted component) − (peak value of the measured component)]/(peak value of the measured component).

3. Results

A. Simulated Test Cases

The results of applying the unmixing algorithm to the example set of eight artificial test cases are summarized in Table 1. In determining the amplitudes of the components, we achieved better than 95% accuracy with as much as a 20% noise level for the test signal. Wavelength location was found to be accurate in all cases except for the weakest pigment emission in the two noise-added cases. Errors of 2 and 3 nm occurred in the 575-pigment location for test cases 7 and 8. Adding a dc offset did not affect the accuracy of the unmixing.

When the algorithm was applied to cases that included pigments in the test data that were not represented in the matrix of prototype spectra, there was a clear mismatch between the unmixing result and the original data in the wavelength region of the missing pigment. Figure 3 shows a test case in which the sample data were a combination of all four pigments but the end member matrix did not include the 575 prototype. This mismatch does not dramatically affect the results for the other pigments.

B. Real Samples

The algorithm was applied to spectra from samples of *Montastrea cavernosa* and *Porites astreoides* that con-

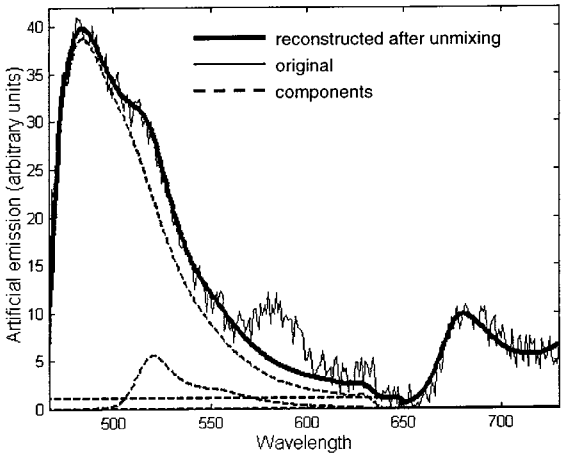

Fig. 3. Artificial test case in which the number of sample pigments exceeds the number of prototype pigments.

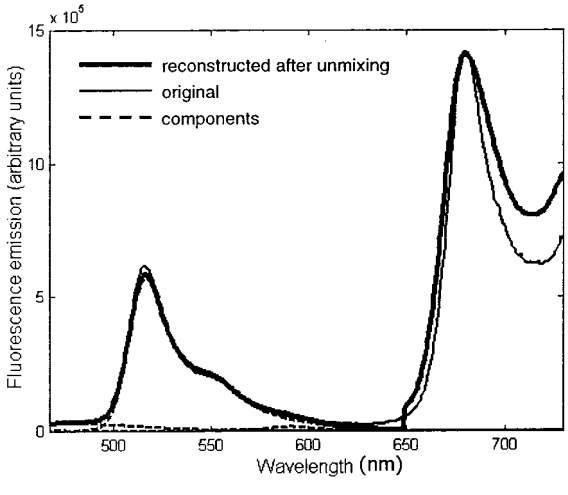

Fig. 4. Measured and reconstructed spectra for *Montastraea cavernosa* specimen with 515 pigment only.

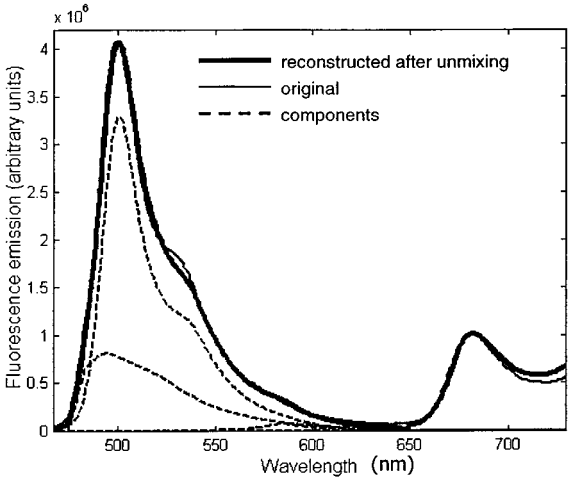

Fig. 5. Measured and reconstructed spectra for *Porites astreoides* specimen with 515 pigment only. Unmixing result is a combination of 486 and 515 pigments.

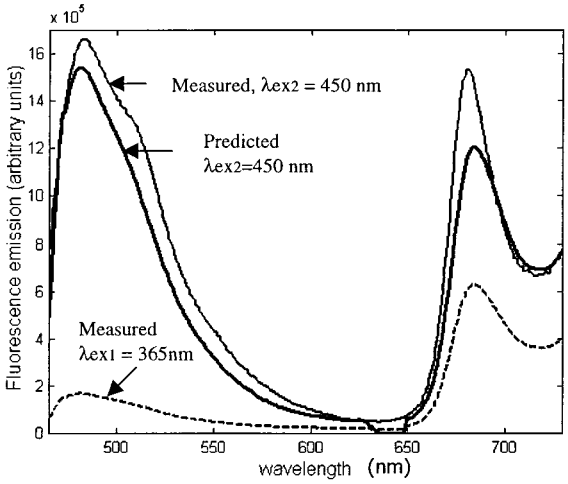

Fig. 7. *Montastraea annularis* specimen with mainly 486 pigment. Sample measured with λ_{ex1} = 365 nm and λ_{ex2} = 450 nm, compared with signal predicted for 450-nm excitation.

tained only the 515 pigment (in addition to chlorophyll) (Figs. 4 and 5). Although the match between the original (thin solid curve) and reconstructed (thick solid curve) spectra was excellent in both cases, the unmixing algorithm indicated that in the latter case there was a significant amount of the 486 pigment present. For a specimen of *Montastrea cavernosa* containing both the 486 and the 515 pigments, the spectrum reconstructed from the unmixed components is nearly identical to the measured spectrum (Fig. 6).

C. Prediction Algorithm

We applied the unmixing and the prediction algorithms to three specimens of *Montastrea annularis* that contained primarily 486 pigment and only a small amount of the 515. The emission spectrum measured with λ_{ex1} = 365 nm was used as the basis for the unmixing and subsequent prediction of the response at λ_{ex2} = 450 nm. The differences between the predicted and the measured 486 peaks were 2.4% (Fig. 7), 3.6%, and 6.7%.

For four specimens of *Montastrea cavernosa* that contained only the 515 pigment the emission spectrum measured with λ_{ex1} = 450 nm was used as the basis for the unmixing and subsequent prediction of the response at λ_{ex2} = 488 nm. The differences between the predicted and the measured 515 peaks were 7.7% (Fig. 8), 8.3%, 8.5%, and 9.9%.

For a specimen of *Montastrea cavernosa* containing significant amounts of both the 486 and 515 pigments, the emission spectrum measured with λ_{ex1} = 365 nm was used as the basis for the unmixing and the subsequent prediction of the response at λ_{ex2} = 450 nm (Fig. 9). For the spectral peak associated with the 486 pigment the difference between the predicted signal and the measured signal was 6.2%. For the peak associated with the 515 pigment the

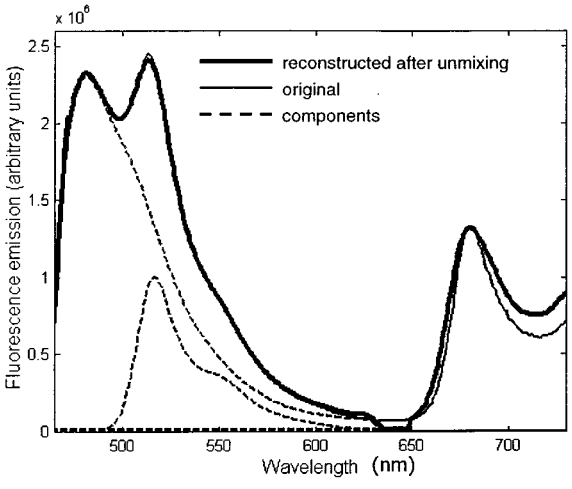

Fig. 6. Measured and reconstructed spectra for *Montastraea cavernosa* specimen with 486 and 515 pigments.

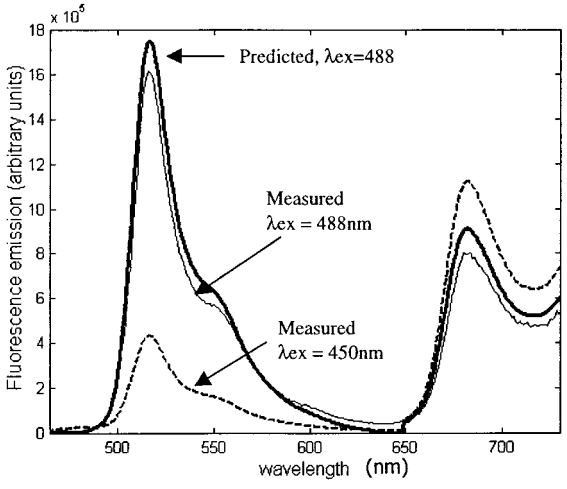

Fig. 8. *Montastraea cavernosa* specimen with 515 pigment only. Sample measured with λ_{ex1} = 450 nm and λ_{ex2} = 488 nm, compared with signal predicted for 488-nm excitation.

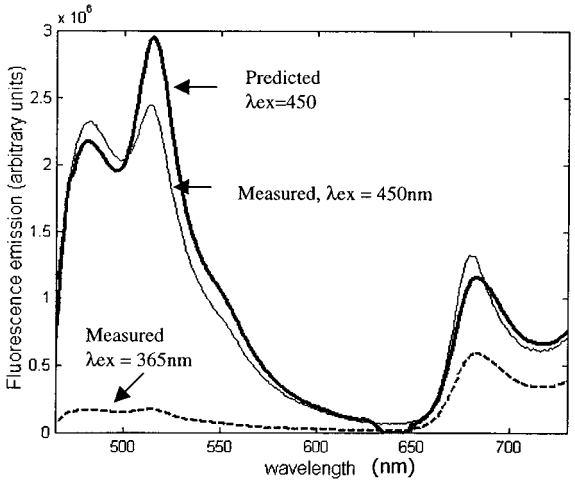

Fig. 9. *Montastraea cavernosa* specimen with 486 and 515 pigments. Sample measured with λ_{ex1} = 365 nm and λ_{ex2} = 450 nm, compared with signal predicted for 450-nm excitation.

difference was 23.2%. For a specimen of *Montastrea annularis* with a similar pigment composition the differences were 1.3% and 39.9%, respectively. In both cases the predicted amplitude of the 515 peak was larger than the measured amplitude. These two specimens were also analyzed with λ_{ex1} = 450 nm and λ_{ex2} = 488 nm. There is no emission from the 486 pigment with 488-nm excitation (Fig. 10). The overprediction of the 515 peak was 147% for the data from *Montastrea cavernosa* and 15% for the specimen of *Montastrea annularis*.

4. Discussion

The least-squares approach to spectral component unmixing is quite standard. The underlying phenomena for the problem addressed here made it necessary to include a provision for the position of the wavelength peaks of the prototype spectra to vary independently over a relatively large spectral range.

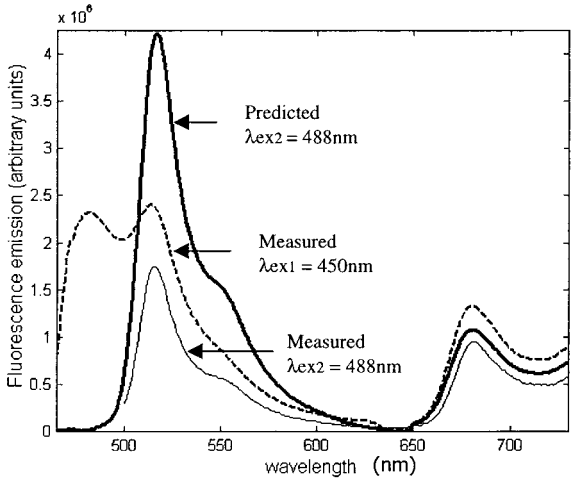

Fig. 10. *Montastraea cavernosa* specimen with 486 and 515 pigments (same as in Fig. 9). Sample measured with λ_{ex1} = 450 nm and λ_{ex2} = 488 nm, compared with signal predicted for 488-nm excitation.

The unmixing algorithm yielded less than 5% error in amplitude in all the simulated data cases shown in Table 1, including test cases with relatively high levels of noise. Wavelength location was accurate except for errors of 2 and 3 nm in the 575-pigment location in the noise-added cases. In those cases the noise amplitudes were 200% and 400% of the amplitude of the 575 component. With low noise levels, an accurate wavelength result was found for all the pigments.

There was consistently good agreement between measured data and curves that were reconstructed from the unmixed components (Figs. 4–6). The most obvious difference between them was in the chlorophyll portion (685 nm) of the emission spectrum. In field samples there is some variability from one specimen to the next in the exact shape of the emission spectrum for any of the pigments.[14] Any mismatch between the spectra of the prototype and the actual pigment in a particular specimen can affect the fit of the final result. A by-product of this spectral mismatch is that the algorithm might indicate the presence of a pigment that was not in the specimen. The addition of a small amount of another pigment could fill in the gap arising from the mismatch. For the case illustrated in Fig. 5 the unmixing algorithm produced an excellent fit but indicated the presence of both 486 and 515 pigments. The measurements for this specimen demonstrated clearly that it contained only the 515 pigment, but a combination of the 486 and 515 prototypes produced a better fit than the 515 alone. The result in this case was also influenced by the extreme shift of the 515 pigment toward the 486 pigment (the peak was at 500 nm).

The practice of setting negative coefficients to zero did not produce any anomalous results. Moving the coefficient away from the value produced by the least-squares operation invariably resulted in an error index that was large enough to ensure that this particular solution would not be the best.

When the sample data contained a pigment that was not represented in the matrix of prototype spectra, the inability of the algorithm to produce a good fit was clear in the result (Fig. 3). The quantitative spectral study of coral fluorescence is still at an early stage, and it is by no means certain that all the pigments that occur in nature have been described spectrally or chemically. Difficulty in application of the unmixing algorithm to field data could be an indicator of the presence of previously undocumented spectral types, thus suggesting that the particular specimen should be examined in greater detail.

The prediction algorithm produced good results when applied to specimens that contained only one pigment in addition to chlorophyll (Figs. 7 and 8) and to the 486 pigment in multipigment samples (Fig. 9). The algorithm overpredicted the 515-pigment component amplitude consistently in cases that contained both the 486 and 515 pigments (Figs. 9 and 10).

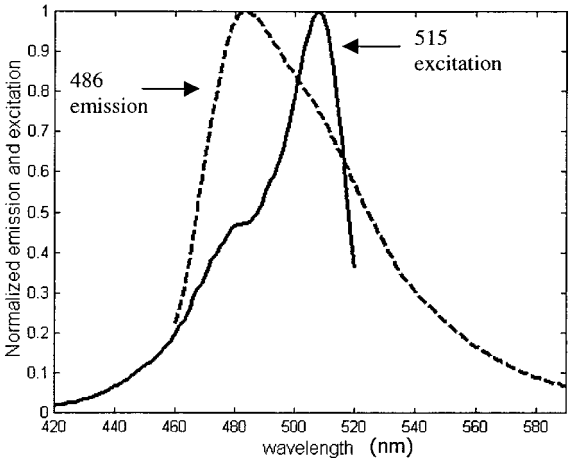

Fig. 11. Overlap between the emission spectrum of the 486 pigment and the excitation spectrum of the 515 pigment (both spectra normalized).

This was not an error in the algorithm, however, but rather arose from fluorescence coupling between the two pigments. There is a significant overlap between the emission spectrum of the 486 pigment and the excitation spectrum of the 515 pigment (Fig. 11). With $\lambda_{ex1} = 450$ nm, the emission from the 515 pigment will arise from two excitation sources: the FluoroMax light source and the emission from the 486 pigment. We know from prior microscopic examinations that the two pigments can occur in close proximity to each other. It is not known whether the coupling is by emission and reabsorption or by resonant transfer. With $\lambda_{ex2} = 488$ nm, the 486 pigment is not excited and emission from the 515 pigment is stimulated only by the instrument light source.

When the program unmixed the spectrum measured with $\lambda_{ex1} = 450$ nm, the 515 component was a combination of two parts: (i) fluorescence excited directly by the instrument light source (em1) and (ii) fluorescence excited by emission from the 486 pigment (em2). When there was no 486 pigment, em2 = 0 and the prediction succeeded (single-pigment cases). Furthermore, the prediction succeeded for the 486 component in both single-pigment and multipigment cases, because there was no coupling between the 515 emission and the 486 excitation. To have no overprediction we would have to apply the prediction algorithm only to the em1 portion of the 515 component. With $\lambda_{ex1} = 365/\lambda_{ex2} = 450$ there was interpigment coupling at both wavelengths.

In principle we could estimate the relative magnitudes of the em1 and the em2 components in the unmixed signal with $\lambda_{ex1} = 450$ nm by applying the prediction algorithm to the case $\lambda_{ex1} = 488/\lambda_{ex2} = 450$ nm. The 515 emission with $\lambda_{ex1} = 488$ nm would not have any coupling, and we should obtain a reasonable prediction of the em1 portion of the 515 component at $\lambda_{ex2} = 450$ nm. The difference between the predicted value and the unmixed value would be the em2 component. From this we could derive an empirical coupling efficiency factor that relates the em2 response to the magnitude of the 486 emission. This could then be used in the analysis of the $\lambda_{ex1} = 365/\lambda_{ex2} = 450$-nm case.

In practice the data we now have are insufficient to address this reliably. The $\lambda_{ex1} = 365/\lambda_{ex2} = 450$-nm case is marginal, because the excitation levels (especially those of the 515 pigment) are quite low,[14] thus making the results quite sensitive to small measurement errors. The multipigment samples that we do have yield quite different values for this empirical coupling efficiency. This in itself is not entirely unexpected. Differences among samples can originate from differences in the fluorescence efficiency of the 515 pigment, the relative physical locations of the 486 and 515 pigments in the coral tissue, concentrations of other light-absorbing substances in the tissues, or the degree of overlap between the 486 emission and the 515 excitation (keeping in mind that the positions of these spectra can vary independently on the wavelength axis). It is hoped that after investigation of additional specimens we can find an empirical coupling efficiency that can be incorporated into the prediction algorithm to account for this secondary fluorescence emission.

Results could also be sensitive to variations in source level or excitation duration. The coral pigments did not change significantly under the illumination conditions used for this experiment. Long exposures to intense illumination could possibly cause photobleaching. If pigments are involved in photochemical activity there could be variations in fluorescence intensity with time, even at moderate illumination levels. This is known to be true for chlorophyll[22] but has not been demonstrated for the coral host pigments.

Our study is part of an ongoing effort to advance the understanding of the nature of the fluorescence signals of corals and to aid in the design and application of *in situ* fluorescence imaging and measurement systems. The addition of more sample spectra to the measurement database will improve the generality of the prototypes used for each of the pigments. The procedures described here will assist in the selection and analysis of field samples and in the intercomparison of results from different measurement systems.

The authors thank Robert Maffione and Jim Bales for helpful comments. This research was supported by the Office of Naval Research, Environmental Optics Program, under contract N00014-97-1-0041.

References

1. C. J. Lorenzen, "A method for the continuous measurement of *in vivo* chlorophyll concentration," Deep-Sea Res. **13,** 223–227 (1966).
2. T. J. Cowles, R. A. Desiderio, and S. Neuer, "*In situ* characterization of phytoplankton from vertical profiles of fluorescence emission spectra," Mar. Biol. **115,** 217–222 (1993).
3. J. Hardy, F. Hoge, J. Yungel, and R. Dodge, "Remote detection of coral bleaching using pulsed-laser fluorescence spectroscopy," Mar. Ecol. Prog. Ser. **88,** 247–255 (1992).

4. J. A. Topinka, K. Korjeff Bellows, and C. S. Yentch, "Characterization of marine macroalgae by fluorescence signatures," Int. J. Remote Sensing **11,** 2329–2335 (1990).
5. S. Kawaguti, "On the physiology of reef corals VI: study on the pigments," Palao Trop. Biol. Stn. Stud. **2,** 617–674 (1944).
6. R. Catala, "Fluorescence effects from corals irradiated with ultra-violet rays," Nature (London) **183,** 949 (1959).
7. K. Shibata, "Pigments and a UV-absorbing substance in corals and a blue-green alga living in the Great Barrier Reef," Plant Cell Physiol. **10,** 325–335 (1969).
8. P. L. Jokiel and R. H. York, Jr., "Solar ultraviolet photobiology of the reef coral *Pocillopora damicornis* and symbiotic zooxanthellae," Bull. Mar. Sci. **32,** 301–315 (1982).
9. D. Schlichter, H. W. Fricke, and W. Weber, "Light harvesting by wavelength transformation in a symbiotic coral in the Red Sea twilight zone," Mar. Biol. **91,** 403–407 (1986).
10. A. Logan, K. Halcrow, and T. Tomascik, "UV excitation-fluorescence in polyp tissue of certain scleractinian corals from Barbados and Bermuda," Bull. Mar. Sci. **46,** 807–813 (1990).
11. L. Delvoye, "Endolithic algae in living stony corals: algal concentrations under influence of depth-dependent light conditions and coral tissue fluorescence in *Agaricia agaricites* (L.) and *Meandrina meandrites* (L.) (Scleractinia, Anthozoa)," Stud. Nat. Hist. Caribbean Region **71,** 24–41 (1992).
12. D. F. Gleason, "Differential effects of ultraviolet radiation on green and brown morphs of the Caribbean coral *Porites astreoides*, Limnol. Oceanogr. **38,** 1452–1463 (1993).
13. C. Mazel, "Spectral measurements of fluorescence emission in Caribbean cnidarians," Mar. Ecol. Prog. Ser. **120,** 185–191 (1995).
14. C. Mazel, "Coral fluorescence characteristics: excitation/emission spectra, fluorescence efficiencies, and contribution to apparent reflectance," in *Ocean Optics XIII*, S. G. Ackleson and R. Frouin, eds., Proc. SPIE **2963,** 240–245 (1997).
15. C. Mazel, "Diver-operated instrument for *in-situ* measurement of spectral fluorescence and reflectance of benthic marine organisms and substrates," Opt. Eng. **36,** 2612–2617 (1997).
16. M. R. Myers, J. T. Hardy, C. H. Mazel, and P. Dustan, "Optical spectra and pigmentation of Caribbean reef corals and macroalgae, Coral Reefs (to be published).
17. M. P. Strand, B. W. Coles, A. J. Nevis, and R. Regan, "Laser line-scan fluorescence and multispectral imaging of coral reef environment," in *Ocean Optics XIII*, S. G. Ackleson and R. Frouin, eds., Proc. SPIE **2963,** 790–795 (1997).
18. A. Savitzky and M. J. E. Golay, "Smoothing and differentiation of data by simplified least squares procedure," Anal. Chem. **36,** 1627–1639 (1964).
19. G. Strang, *Introduction to Applied Mathematics* (Wellesley-Cambridge Press, Wellesley, Mass., 1986).
20. J. J. Settele and N. A. Drake, "Linear mixing and the estimation of ground cover proportions," Int. J. Remote Sensing **14,** 1159–1177 (1993).
21. C. D. Mobley, *Light and Water* (Academic, San Diego, Calif., 1994).
22. J. C. Goedheer, "Fluorescence in relation to photosynthesis," Ann. Rev. Plant Physiol. **23,** 87–112 (1972).